Test and Analysis of 4 Technology Quadrupole Shell (TQS) models for LARP

S. Caspi, G. Ambrosio, A.N. Andreev, E. Barzi, R. Bossert, D. R. Dietderich, H. Felice, P. Ferracin, A. Ghosh, A. R. Hafalia, A. F. Lietzke, I. Novitski, G.L. Sabbi, and A.V. Zlobin

***Abstract*—Test results are reported on TQS02a, a second model in support of the development of a large-aperture Nb_3Sn superconducting quadrupole for the US LHC Accelerator Research Program (LARP). The magnet uses key and bladder technology with supporting iron yoke and an aluminum shell. Changes from the previous first model (tested in 2006) include:1) Titanium island poles 2) no axial island gaps during reaction and 3) RRP Nb_3Sn conductor. Design changes resulted from previous tests with three different magnet assemblies (TQS01a, TQS01b and TQS01c) using coils with bronze segmented islands, with gaps and MJR conductor The paper summarizes the assembly, cool-down and performance of TQS01a, TQS01b, TQS01c, and TQS02 and compares measurements with design expectations**

***Index Terms*— LARP, Nb_3Sn, Superconducting Quadrupole Magnet, TQS.**

I. INTRODUCTION

THE Technology Quadrupole (TQ) magnet series, under development by the U.S.-LHC Accelerator Research Program (LARP), is a close partnership between magnet physicists and engineers from BNL, FNAL and LBNL [1]. The program long term goal is to demonstrate, by the year 2009, that Nb_3Sn magnets are a viable choice for an LHC IR upgrade [2]. A successful test will have to demonstrate a 3.6 m long magnet with a 90 mm bore and a gradient above 200 T/m. Over the past three years several steps in that direction were taken. A Subscale Quadrupole magnet program (SQ) [3] was lunched to study small Nb_3Sn racetrack coils, a Technology Quadrupole (TQ) program extended the SQ technology to 1 m long cos-theta coils and the Long Racetrack program (LR) [4] extended the same technology to 3.6 m long coils. The Long Racetrack program had recently successfully tested a magnet (LRS01) using two Nb_3Sn racetrack coils assembled as "common coils" within a shell structure pre-stressed using "keys and bladders" technology [5].

At the present time the LARP TQ program is using a parallel path of two different structures to test virtually identical coils. The LBNL approach (TQS) [6]-[9] is to use a shell-based structure with "keys and bladders" assembly (see Fig. 1 and Fig. 2), while the FNAL approach (TQC) [10], [11] is to use a collar-based structure, applying a modified NbTi assembly procedure, to the assembly of Nb_3Sn coils.

Fig.1. An assembled TQS magnet ready for testing. Showings are the outer aluminum shell, end-plate, and four axial rods.

This paper focuses on the recent test results of magnet TQS02a. It also summarizes and compares test results of 4 different TQS assemblies in an attempt to address technological issues and provide guidance to future tests.

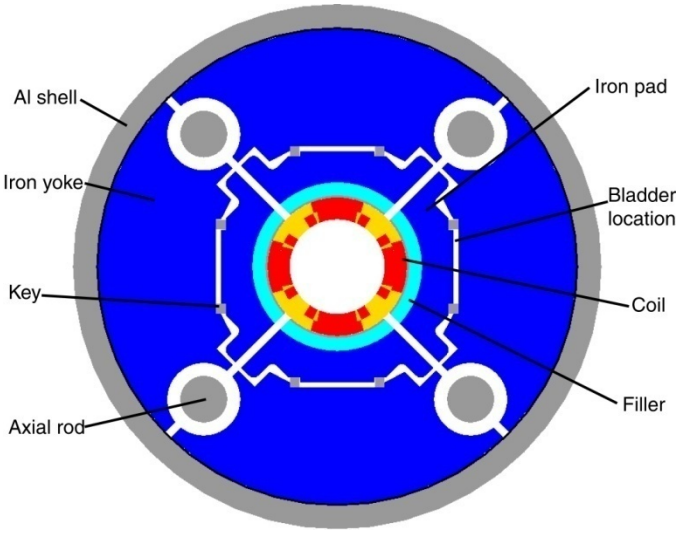

Manuscript received August 28, 2007. This work was supported by the Director, Office of Energy Research, Office of High Energy and Nuclear Physics, High Energy Physics Division, U. S. Department of Energy, under Contract No. DE-AC02-05CH11231

S. Caspi, D.R. Dietderich, P. Ferracin, A.R. Hafalia, A.F. Lietzke and G.L. Sabbi are with Lawrence Berkeley National Laboratory, Berkeley, CA 94720 USA (phone: 510-486-7244; fax: 510-486-5310; e-mail: s_caspi@lbl.gov).

G. Ambrosio, A.N. Andreev, E. Barzi, R. Bossert, I. Novitski and A.V. Zlobin, are with Fermi National Laboratory, Batavia, IL 60510-0500 USA.

A. Ghosh is with Brookhaven National Laboratory, Upton, NY 11973-5000 USA.

II. Fig. 2. TQS magnet cross-section showing coils, fillers, pads, keys, yokes, skin and axial supporting rods. Magnet Design

A. Conceptual design and parameters

The shell-based structure approach uses bladders and keys for precise room temperature pre-stress control, with negligible stress "overshoot" during magnet assembly. Interference keys are inserted to retain the pre-stress and allow bladder removal. A tensioned aluminum shell compresses internal iron and coil components, and applies a substantial fraction of the operational pre-stress during cool-down. Accordingly, the final coil pre-stress is monotonically approached from below, without overstressing the fragile conductor [12]. Design parameters are shown in Tables I

The magnet design and analysis went through several iterations using three major computer programs: ProE (CAD), TOSCA (magnetic analysis), and ANSYS (structural analysis). Three dimensional analysis was used throughout and in the structural analysis a friction factor (μ) was included between components. A friction factor of μ=0.2 was used between all coil surfaces and μ=0.5 between the shell and the yoke. The results 1) provided a target room-temperature azimuthal and axial assembly pre-stress, 2) predicted the cool-down impact on pre-stress, and 3) estimated axial and azimuthal response during excitation. The target specs for the magnet pre-stress at 4.4 K was to prevent possible coil-island separation in the straight section and the ends.

Based on an extensive ANSYS study, an applied shell stress around 170 MPa and an applied axial force of approximately 800 kN (at 4.4 K) were needed to overcome frictional and Lorentz forces and prevent coil-island separation. This was accomplished azimuthally by an aluminum shell, and axially by four aluminum tie-rods pulling stainless steel end plates against coil-end shoes. In the TQS01 series of magnet tests, only 30% of that force was actually needed to be applied during assembly, the rest was reached during cool-down by the contracting aluminum shell and tie rods. In contrast, during the TQS02a assembly less than 15% was needed to be applied. According to the computations, the applied cold axial force had to be more than twice that of the maximum Lorentz force to overcome frictional forces. To minimize the influence of friction during assembly pre-stress was first applied axially and then azimuthally.

B. Strain gauges

The use of strain gauges was essential in determining the stress conditions in the coils and structure. They have also been a key element providing measured response to ANSYS modeling and analysis. Each of the 4 coils was instrumented with strain gauges mounted on the inner surface of the islands (aluminum-bronze or titanium alloy). On the islands, at their axial center, two gauges were mounted to measure the azimuthal and axial strain, and an additional axial gauge was placed near the lead-end. All island gauges were compensated computationally against gauges mounted on free island material.

Measured strain "ε" in two principal directions "z, θ" (and no shear) was converted into stress "σ" using the relationships below assuming a *modulus of elasticity* E, and *poisson's ratio* ν for bronze or titanium (islands) and aluminum (shell or rods) (Table II),

$$\sigma_\theta = \frac{E}{(1-\nu^2)}(\varepsilon_\theta + \nu\varepsilon_z) \quad \sigma_z = \frac{E}{(1-\nu^2)}(\varepsilon_z + \nu\varepsilon_\theta)$$

TABLE I TQS Magnet Parameters

	Unit	Magnet Parameters
Strand Diameter	mm	0.7
N strands		27
Mid-thickness bare	mm	1.26 ± 0.02
Width bare	mm	10.06 ± 0.05
Keystone angle	Degree	1.05 ± 0.1
Insulation thickness	mm	0.125
Turns per block		6+12 layer 1, 16 layer 2
mandrel diameter	mm	90
Shell thickness	mm	22
Shell outer diameter	mm	500

TABLE II Material Properties used in ANSYS

ANSYS	Modulus (GPa) 300 K	Modulus (GPa) 4.4 K	Poisson Ratio	Thermal Expansion 300k -4.4K
Aluminum	70	79	0.34	-0.00420
Bronze	110	120	0.30	-0.00312
Iron	213	224	0.28	-0.00197
Titanium	130	130	0.30	-0.00174
Conductor	45	-45	0.20	-0.00336

C. Assembly and cool-down

The magnet was assembled from two sub-assemblies: a coil pack of four coils held together by four adjustable load-pads to ensure uniformity, and a structure pack of four iron yokes separated temporarily by gap-keys and held by an outer aluminum shell. During final assembly the gap-keys between the yokes were removed and replaced by interference keys inserted between pads and yokes using pressurized bladders. The coils were pre-stressed azimuthally and axially. While holding the coils snuggly within the structure, an axial end-force was applied to the coil ends by tensioning the four tie-rods. Azimuthal pre-stress was then applied using keys and bladders. The final room temperature coils pre-stress was approximately -40 MPa azimuthally and -20 MPa axially

III. TQS01 and TQS02

The three TQS01 tests (a,b,c) used coils with segmented bronze islands and MJR conductor. Except TQS01a, which used virgin coils, tests b and c combined virgin and previous tested recycled coils. Small adjustments to pre-stress and friction factors were made with inconclusive or little impact on the magnet performance. During all three tests quench origins concentrated around the first pole-turn near the gap between segmented islands. Gaps between segmented islands were introduced intentionally to prevent excessive strain on the conductor during reaction. Total gaps of about 2 mm were maintained during impregnation. Based on the TQS01 test results and additional detailed ANSYS analysis, a decision was made to replace the bronze islands with titanium islands, with the goal of eliminating the need for any intentional gaps during reaction and leaving the island compressed axially after

cool-down. That change was implemented in TQS02a.

The choice of no island gaps in TQS02a proved to be successful when after the reaction no separating gaps between segments could be seen and the coil ends remained attached to the end spacers and shoes (the "best looking" coils as quoted by the technicians). The coil conductor was RRP with a measured RRR around 200, a Cu to NonCu ratio of 0.87 and a current density around 2740 A/mm^2 at 12 T, 4.2 K as measured on an extracted strand (assuming no self field correction).

The calculated stress and strain in magnets TQS01 and TQS02 are summarized in Tables III, IV. Warm and cold data are listed for the shell, rods, islands, and pole turn 1 around the island.

TABLE III TQS01 STRESS-STRAIN - CALCULATIONS

ANSYS	STRESS (MPa)		STRAIN (με)	
	300 K	4.4 K	300 K	4.4 K
Shell azimuthal	+30	+166	+380	+1495
Shell axial Z	+9	+142	-19	+1080
Rods axial Z	+37	+128	+527	+1618
Island azimuthal θ	-50	-220	-340	-1890
Island axial Z	-43	+25	-250	+765
Turn 1 (layer 1) θ	-40	-155	-780	-3450
Turn 1 (layer 1) z	-20	+12	-250	+1000

TABLE IV TQS02 STRESS-STRAIN - CALCULATIONS

ANSYS	STRESS (MPa)		STRAIN (με)	
	300 K	4.4 K	300 K	4.4 K
Shell azimuthal	+29	+178	+373	+1611
Shell axial Z	+9	+148	-18	+1115
Rods axial Z	+15	+110	+208	+1398
Island azimuthal θ	-50	-131	-350	-830
Island axial Z	-17	-77	-18	-290
Turn 1 (layer 1) θ	-39	-155	-789	-3350
Turn 1 (layer 1) z	-10	+12	-19	+1312

IV. TEST RESULTS

A. Training

The training curve for the 4 tests is shown in Fig. 3. At 4.4 K the TQS01 magnets reached their plateau values in less than a dozen quenches with a maximum current between 82%-87% of the expected magnet short sample [13]-[14] and a maximum gradient just short of 200 T/m. TQS02a trained slower, reaching a gradient plateau of 215 T/m at 4.4 K and a maximum current of 92% of short sample (without self field correction). Training at 1.9 K proved to be different. Whereas TQS01c has gained about 1000 A at 1.9 K (as expected, and after a long training process) TQS02a did not. Except for sporadic and erratic gains, TQS02a remained unchanged with a onetime maximum gradient of 225 T/m at 2.17 K [15].

The slow or no gain in magnet current at 1.9K remains unexplained. We note that, on the one hand, after magnet disassembly coils tested only at 4.4 K had no visible signs of high stress or strain. On the other hand, coils tested at 1.9K were left with several dozen of round marking on all of the inner layer coils. Such marking, on the free unsupported bore surface, were also observed in the FNAL TQC01 test. Our explanation suggests that the marking, resembling flat "bubbles" (Fig. 4), are created during a quench when superfluid that has penetrated into small "super-cracks" within the epoxy could not escape as the quench temperature rises. As a result of a transition to vapor and a build-up of high local pressure, repeated quenches may weaken the cracks near the free surface causing them eventually to break through and damage the insulated glass. It is unclear what is the impact of the "bubbles" on the magnet performance but they are most likely not the cause of a quench but rather an after affect. However what the "bubbles" may be telling us, indirectly, is that impregnated coils are not hermetically sealed, they are full of micro-cracks that change in size as the magnet is energized and trained. That implies a substantial source of energy release mechanism that needs to be avoided. Better impregnation and additional copper within strands may help; however, additional short-sample tests of impregnated cable may shed light on what we see on unsupported surfaces.

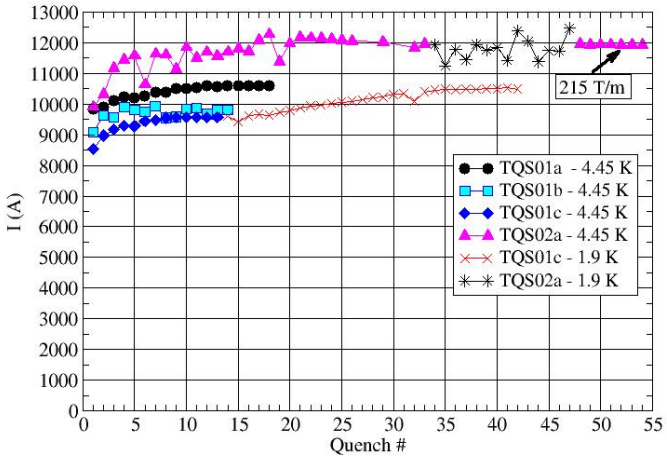

Fig.3. Training curves of the 4 test TQS magnets.

A second unusual observation was associated with quench locations in TQS02a. A large number of quenches originated in the outer layer, a rather unusual event given the fact that the field there is at least 1T lower than the inner layer. Since all outer layer quenches occurred in one coil only (coil 21) we can only speculate that there must have been something peculiar about that coil. The last unusual phenomenon observed during the TQS02a test is with regard to the maximum current, which was reached at 2.17 K.

Fig.4. Several "bubbles" as they appear after a 1.9K test of TQS02a.

B. Strain measurements

The operational pre-stress was reached during cool-down. Differences in the thermal contraction properties between aluminum and iron continued to increase pre-compression in the coils. Fig. 5 shows a typical time sequence of measured strain in the TQS02a axial rods from assembly through testing and disassembly. Similar curves are recorded for the shell and islands. Whereas the rods and the shell only marginally respond to an increase in magnet current, the island gauges reflect (as expected) a decrease in coil stress on the pole.

When the magnet is energized, the azimuthal and axial

stresses in the islands respond linearly to the Lorentz force correspondingly as a function of the current square (Fig. 6). Whereas the azimuthal stress in TQS01c and TQS02a are practically overlapping, as expected the TQS01c bronze island is under tension while the TQS02a titanium island is under compression. A departure from a strictly linear behavior is also visible at high currents. Tables V and VI list measured strain-stress at 300 K and 4.4 K. Most of the measured data agrees with ANSYS calculations.

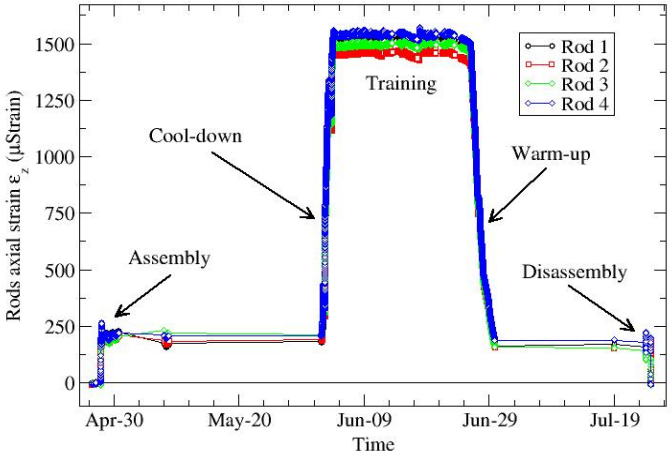

Fig.5. Measured strain of TQS02a rods during assembly, testing and disassembly.

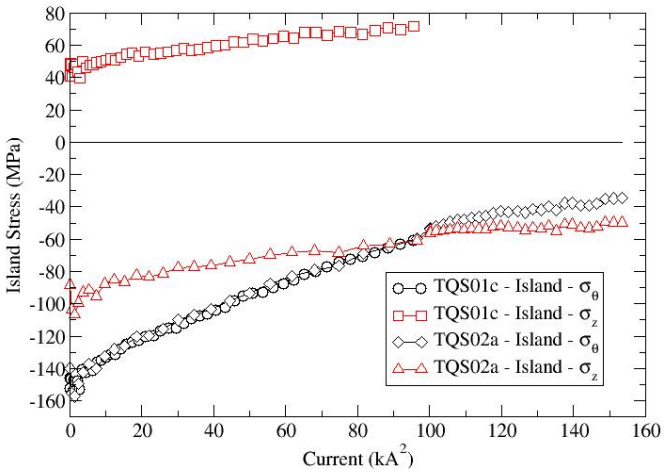

Fig.6. Measured island stress in TQS01c and TQS02a.

TABLE V MEASURED STRAIN-STRESS AT 300K

			Measured TQS01a	TQS01b	TQS01c	Measured TQS02a
με	Shell Strain	ε_θ	+465	+620	+360	+335
με	Shell Strain	ε_z	0	0	-25	-58
MPa	Shell Stress	σ_θ	+42	+55	+31	+28
MPa	Shell Stress	σ_z	+14	+19	+9	+5
με	Rods Strain	ε_z	+555	+550	+600	+196
MPa	Rods Stress	σ_z	+44	+44	+47	+16
με	Island Strain	ε_θ	-150	-172	+15	-174
με	Island Strain	ε_z	-63	-178	-150	-12
MPa	Island Stress	σ_θ	-22	-30	-4	-25
MPa	Island Stress	σ_z	-14	-30	-27	-9
με	Pole turn Strain	$\varepsilon_\theta, \varepsilon_z$			Not measured	
MPa	Pole turn Stress	σ_θ	-18	-24	-3	-19
MPa	Pole turn Stress	σ_z	-7	-14	-13	-5

C. *Magnetic measurements*

The measured dodecapole (b_6 at R_{ref}=21 mm) for TQS01c and TQS02a is shown in Fig. 7. The data for both magnets overlaps and is in close agreement agrees with expected calculations. Additional magnetic measurements details are available in [16].

TABLE VI MEASURED STRAIN-STRESS AT 4.4K

			Measured TQS01a	TQS01b	TQS01c	Measured TQS02a
με	Shell Strain	ε_θ	+1325	+1456	+1275	+1379
με	Shell Strain	ε_z	+1154	+1073	+1110	+1108
MPa	Shell Stress	σ_θ	+153	+163	+148	+157
MPa	Shell Stress	σ_z	+143	+140	+138	+141
με	Rods Strain	ε_z	+1435	+1475	+1880	+1499
MPa	Rods Stress	σ_z	+113	+117	+149	+118
με	Island Strain	ε_θ	-1733	-1771	-1450	-918
με	Island Strain	ε_z	+776	+792	+730	-347
MPa	Island Stress	σ_θ	-198	-202	-162	-146
MPa	Island Stress	σ_z	+34	+34	+39	-89
με	Pole turn Strain	$\varepsilon_\theta, \varepsilon_z$			Not measured	
MPa	Pole turn Stress	σ_θ	-139	-142	-114	-150
MPa	Pole turn Stress	σ_z	+15	+15	+17	+48

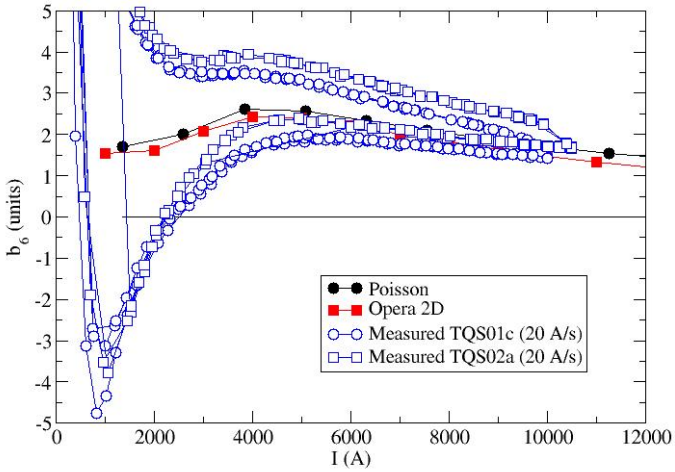

Fig.7. Measured dodecapole for TQS01c and TQS02a.

V. HEATER STUDIES

One coil in magnet TQS01c (coil 15) was intentionally sacrificed to test the impact of heating during a quench on coil performance [17]. Spontaneous quenches at 4.4 K were used during this study with increasing dump delays (up to 200 ms) to bust up the magnet MIITs. Standard current ramps with no dump delay were performed after each MIITs deposition in order to asses any changes in magnet performance. Fig. 8 shows a deteriorated current plateau as the MIITs are raised beyond 8. Damage to coil 15 was also noted by the island gauges showing sever reduction in its azimuthal stress and ratcheting (Fig. 9). Upon magnet disassembly physical damage could clear be seen all along the inner first two turns along one side of the island (Fig. 10).

VI. CONCLUSION

Four magnets were tested using a shell based structure with keys and bladder assembly procedure. Stress measurements of the coils and structure were closely followed with program ANSYS. The magnets trained and reached a plateau between 82-92% of the expected short-sample limit. Replacing the bronze islands with titanium eliminated quench origins from reoccurring near segmented gaps and also eliminated the need for any intentional gaps between segments. TQS02a, with

improved RRP conductor, reached a stable gradient of 215 T/m at 4.4 K and the potential of reaching even higher levels as seen by a single quench of 225 T/m at 2.17 K. Issues regarding the 1.9 K performance and outer layer quenches will need further studies.

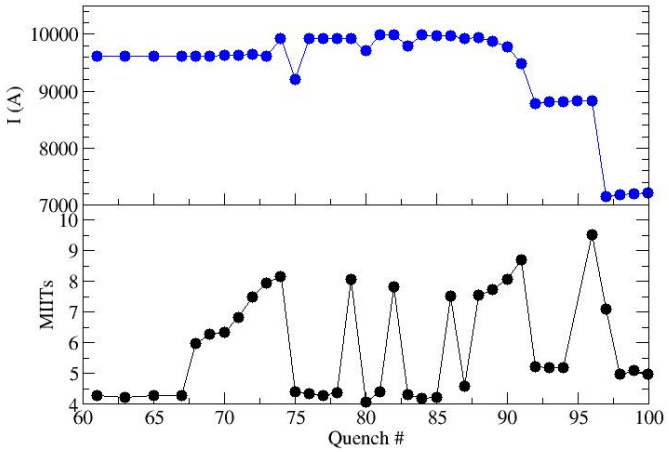

Fig.8. Heater studies in magnet TQS01c.

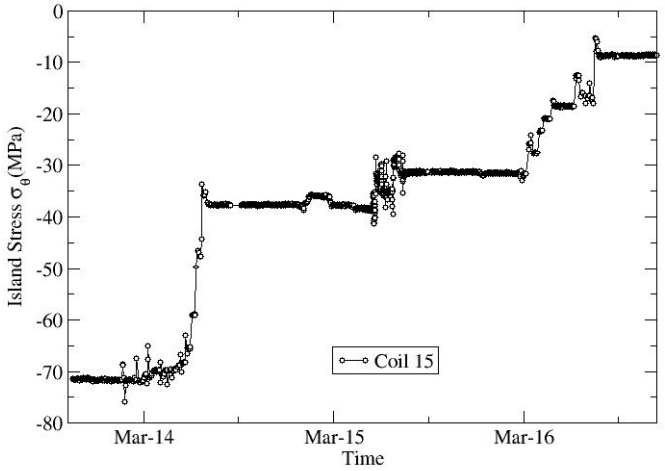

Fig.9. Permanent ratcheting during heater studies measured by strain gauges

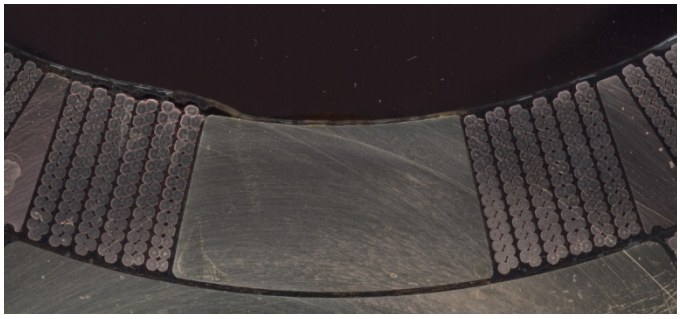

Fig.10. Visible damage to coil 15 after MIITs heater study.

ACKNOWLEDGMENT

We thank our technical staff for their expertise, hard work and dedication.

REFERENCES

[1] S.A. Gourlay, *et al.*, "Magnet R&D for the IS LHC Accelerator Research Program", *IEEE Trans. Appl. Supercond.*, vol. 16, no. 2, June 2006, pp. 324-327.

[2] G. Sabbi *et al.*, "Nb3Sn quadrupole magnets for the LHC IR", *IEEE Trans. Appl. Supercond.*, Vol. 13, no. 2, June 2003, pp. 1262-1265.

[3] P. Ferracin, *et al.*, "Assembly and Tests of SQ02, a Nb_3Sn Racetrack Quadrupole Magnet for LARP", *IEEE Trans. Appl. Supercond.*, vol. 17, no. 2, June 2007, pp. 1019-1022.

[4] P.J. Wanderer, *et al.*, "Construction and Test of 3.6 m Nb3Sn Racetrack Coils for LARP", paper 3E03 this conference.

[5] P. Ferracin, *et al.*, "Assembly and Test of a Support Structure for 3.6 m Long Nb_3Sn Racetrack Coils", paper 3E02 this conference.

[6] S. Caspi, *et al.*, "Mechanical Design of a Second Generation LHC IR Quadrupole", *IEEE Trans. Appl. Supercond.*, Vol. 14, no. 2 June 2004, pp. 235-238.

[7] S. Caspi, *et al.*, "The use of pressurized bladders for stress control of superconducting magnets", *IEEE Trans. Appl. Supercond.*, Vol. 11, no. 1, March 2001, pp. 2272-2275.

[8] A. R. Hafalia, *et al.*, "A new support structure for high field magnet", *IEEE Trans. Appl. Supercond.*, Vol. 12, no. 1, March 2002, pp. 47-50.

[9] A. R. Hafalia, *et al.*, "Structure for an LHC 90 mm Nb_3Sn quadrupole magnet", *IEEE Trans. Appl. Supercond.*, Vol. 15, no. 2, June 2005, pp. 1444-1447.

[10] R.C. Bossert, *et al.*, "Development of TQC01, a 90 mm Nb_3Sn model quadrupole for the LHC upgrade based on SS collars", *IEEE Trans. Appl. Supercond.*, vol. 16, no. 2, June 2006, pp. 370-373.

[11] S. Feher, *et al.*, "Development and Test of LARP Technological Quadrupole (TQC) Magnet", *IEEE Trans. Appl. Supercond*, vol. 17, no. 2, June 2007, pp. 1126-1129.

[12] S. Caspi, *et al.*, "Design and analysis of TQS01, a 90 mm Nb_3Sn model quadrupole for the LHC luminosity upgrade based on a key and bladder assembly", *IEEE Trans. Appl. Supercond.*, vol. 16, no. 2, June 2006, pp. 358-361.

[13] S. Caspi, *et al.*, "Fabrication and Test of TQS01 – a 90 mm Nb_3Sn Quadrupole Magnet for LARP", *IEEE Trans. Appl. Supercond*, vol. 17, no. 2, June 2007, pp. 1122-1125.

[14] E. Barzi, *et al.*, "RRP Nb_3Sn Strand Studies for LARP", *IEEE Trans. Appl. Supercond.*, vol. 17, no. 2, June 2007, pp. 2607-2610.

[15] G. Ambrosio, *et al.*, "LARP TQS02a Test Summary", FNAL report TD-07-0xx, 8/8/07.

[16] G.V. Velev, *et al.*, "Field Quality Measurements and Analysis of the LARP Technology Quadrupole Models", paper 3E06 this conference.

[17] G. Ambrosio, *et al.*,"TQS01c Test Summary", FNAL report TD-07-0xx, 3/29/07.